

Feasibility of a Braided Composite for Orthopedic Bone Cast

Katherine R. Evans and Jason P. Carey*

4-9 MecE building, University of Alberta, Edmonton, Alberta, Canada, T6G 2G8

Abstract: A tubular braided composite bone cast for improving the efficiency and quality of bone fracture treatment is investigated. Finite element analysis was used to evaluate stress concentrations in fracture sites supported with plate and tubular casts. The stress in a plated bone is 768 % of that in a whole bone at the same location, while it is only 47 % in a bone with a tubular cast. Three unbroken synthetic humeri were mechanically tested using an in-vitro long bone testing procedure developed in-house to find their stiffness at 20° and 60° abduction; these were found to be 116.8 ± 1.5 N/mm and 20.63 ± 0.02 N/mm, respectively. A 2 cm gap osteotomy was cut through the diaphysis in each bone. The bones were casted with a Kevlar/Cold cure composite, with calculated braid angles and thicknesses that closely matched bone properties. The stiffness tests were repeated, and the results were within 10 % of the unbroken bone. This novel method of bone casting is promising if other clinical challenges can be minimized.

Keywords: Analogue humerus, bone model, braid, composite, finite element analysis (FEA), non-destructive testing, stiffness.

INTRODUCTION

Diaphyseal bone fracture in a long bone is typically stabilized using stainless steel, cobalt-chromium and titanium plates and bone grafts to allow union between the fractured portions of the bone [1]. The use of metal plates leads to stress shielding, in which stresses placed on the bone are supported by the stiff metal plate, leading to insufficient physiological loading on the bone. This causes bone resorption and osteoporosis [2–4]. This is in accordance with Wolff's law, which states that without loading, a bone will become weaker and less dense [5]. As a result, refractures can occur if the plate is removed [6]. Alternatively, it has been suggested that high shear stiffness is desirable to improve healing [7, 8]. While this is true of metal, the high stiffness in tension and compression is undesirable. Stiffness that is too low can result in micro-movements of the fractured bone segments, which is also undesirable. Thus, stiffness similar to that of human cortical bone is ideal [9]. Other problems include screw damage to healthy bone, abnormal bone loading, nerve damage, and muscle trauma [10]. Metal plates also cause problems with imaging using X-Ray, computed tomography, or magnetic resonance imaging, making interpretation difficult or even impossible [5, 9]. As well metal alloys can cause an allergic reaction in some patients [11]. Secondary surgeries are often required to replace, repair, or remove the internal fixation, resulting in increased health care costs, longer wait times, and decreased patient comfort.

Composite materials can have similar properties, such as stiffness, strength, and anisotropy, to soft and hard tissues [12]. This reduces the stress shielding effect and promotes more effective bone repair [2-4]. Thus composite

compression bone plates have been investigated to overcome some of the difficulties mentioned. Composite materials can easily be imaged, and are less susceptible to corrosion than metal alloys [12]. Short fiber composites have been studied, but have produced relatively poor mechanical properties [13]. Unidirectional laminates are used to reinforce composites [2, 3], but have low strength and stiffness in the two directions perpendicular to the fibers [13]. As well, load-carrying abilities are decreased potentially due to splitting along the plate axial direction [9]. Three dimensional composites provide balanced properties in various directions [13]. Studies into knitted fabric composites have been conducted, producing composite bone plates with Young's Moduli close to that of cortical bone [11, 14, 15]. In each case fiber discontinuity at screw holes weakens the composite, screw damage occurs, and secondary surgeries may still be required [9].

A shape adaptable composite braid that wraps entirely around the bone fracture site could be used to eliminate the need for screws. The braid would be compact, but have enough room to be collapsed inwards, as with a classic finger trap. When collapsed, the braid preform would expand allowing it to be easily slipped between the broken ends. Once in place it would be stretched to bridge the fracture gap, as shown in Fig. (1). Because a braid is continuous there would be an even stress distribution which would result in more uniform healing. It would be able to contain small bone fragments, which could help with the healing process, and could be tailored to have optimal stiffness. The braid could be thinner than a plate, which is desirable due to the limited space between muscle and bone [14]. Mechanical properties of bone depend on various factors such as age, gender, lifestyle, shape, and sustained physiological loading, so a patient specific cast is ideal [15]. A fully resorbable bone setting system is desirable, as this would eliminate a potential secondary surgery to remove the cast and improve

*Address correspondence to this author at the 4-9 MecE building, University of Alberta, Edmonton, Alberta, Canada, T6G 2G8; Tel: 780-492-7168; Fax: 780-492-2200; E-mail: jpcarey@ualberta.ca

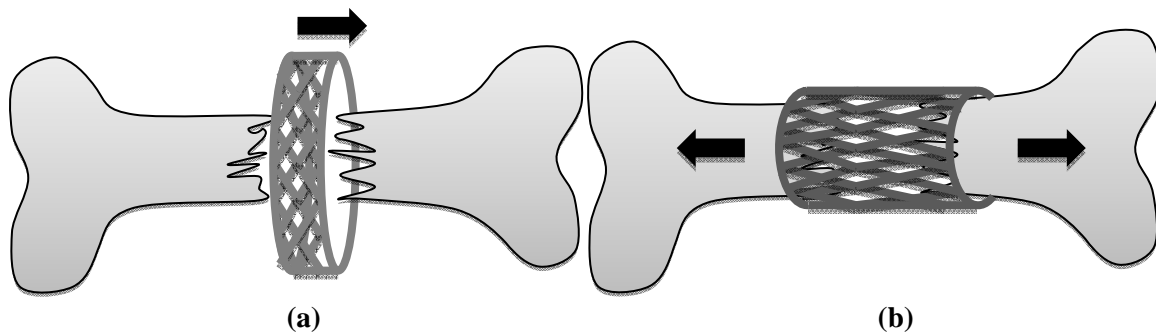


Fig. (1). Broken bone with (a) expanded braid inserted, and (b) braid stretched to cover the broken ends.

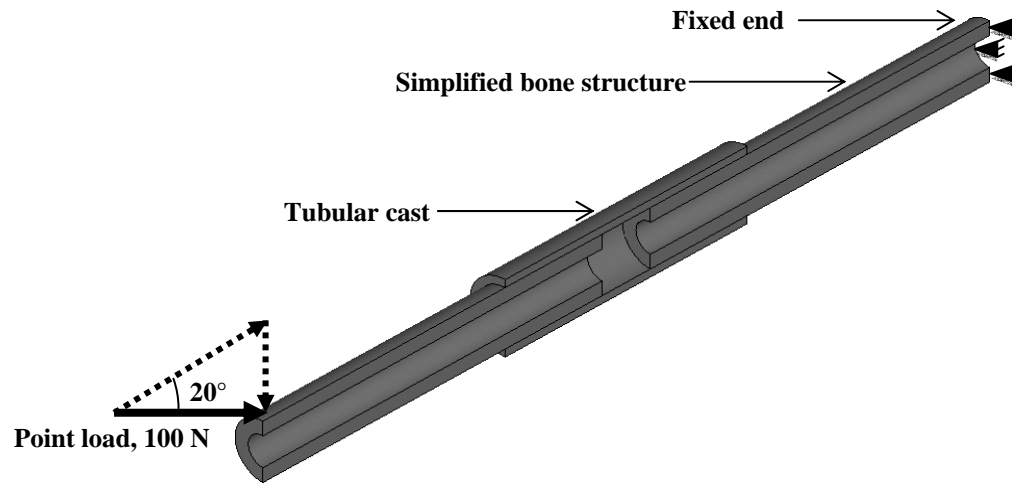


Fig. (2). Tubular casted bone model set-up for FEA.

patient comfort. Braid edges could be sectioned to allow to wrap or contour muscle attachments, nerve and vascular areas.

This project is part of a larger research program underway to develop near patient specific braided casts based on computed tomography or magnetic resonance images, optimized computer aided design bone reconstruction and rapid prototyping and selection of braid geometry and production variables to match bone properties. The objective of this investigation was to demonstrate the proof of this concept with synthetic bones. It was hypothesized that the cast would give the broken bone properties similar to normal bone.

MATERIALS AND METHODS

Finite Element Analysis Comparing Plate and Tubular Supports

The difference in stress between plate and tubular supports was investigated. It was hypothesized that the maximum stress in the bone under a braided cast would be much smaller than that produced by a bone plate. This was checked using simple Finite Element Analysis (FEA) in pure bending, with one side of the bone fixed and a point load of 100 N applied to the other side at an angle of 20° abduction from the bone longitudinal axis to mimic simple physiological loading conditions of approximately supporting a 10kg mass. The set-up is shown in Fig. (2).

For simplicity and representative structure, a hollow cylinder was selected due to the high ratio of stiffness

between the cortical and cancellous bone, resulting in the cortical bone supporting most of the stress, thus rendering the effects of the cancellous bone negligible. The bone was approximated from the dimension of a fourth generation Sawbones (Pacific Research Laboratories, Inc., Washington, USA) humerus model 3403 as a 300 mm long half cylinder with an outer diameter of 23 mm and inner of 12 mm, with symmetrical constraints applied. The length was chosen to approximate the diaphysis of a humerus. The break distance was chosen to be 20 mm, classified as a highly comminuted fracture, such as a Type B3, C1, or C3 based on the Swiss Association for the Study of Problems of Internal Fixation (AO) classification, and as such likely to require internal fixation [16]. The thickness of the plate and tube were set to 3 mm, and both were fixed to the bone by connecting nodes to simulate a completely attached cast; screws were not simulated in this simplified model. Constant cortical bone properties were assumed for both the bone and the cast, as determined by Ashman *et al.* [17].

ANSYS was used to complete the analysis. Each bone was meshed automatically using element type SOLID186. This 20-node solid element was selected since it exhibits quadratic displacement behavior and each node has the desirable degrees of freedom: translation in the x -, y -, and z -directions. As well the element type allows anisotropic material properties. A mesh dependency analysis on maximum von Mises stress and displacement in the bone was conducted for the plated bone. Both the maximum displacement and Von Mises stress graphs show a

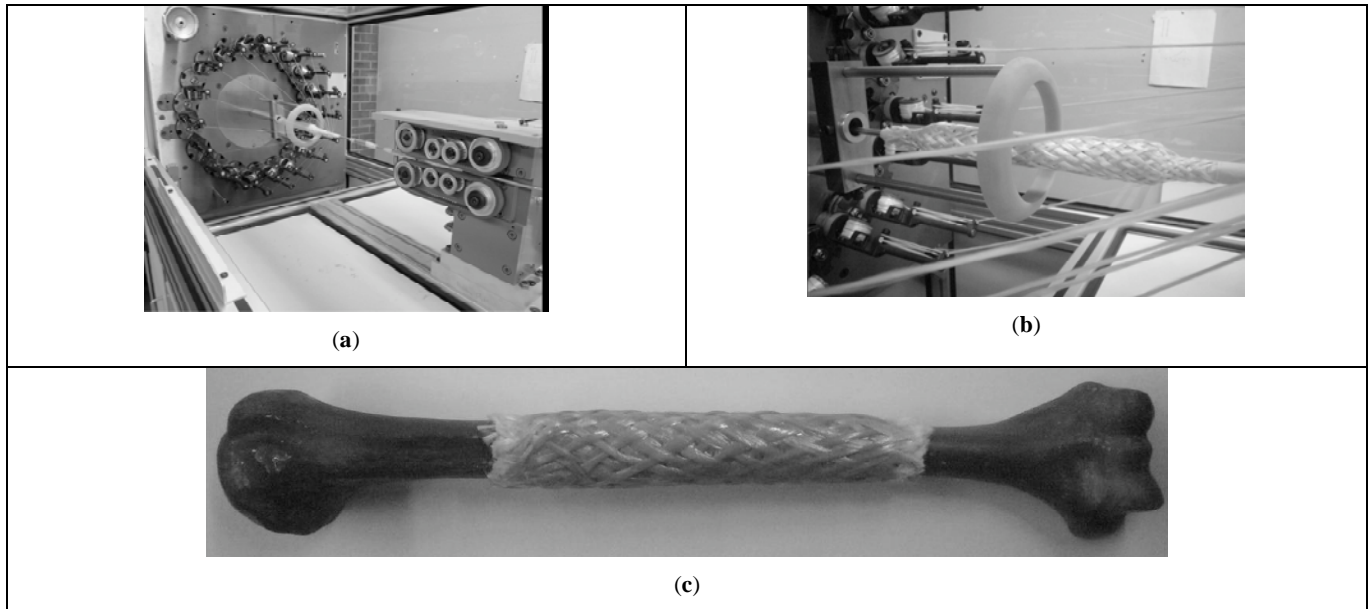


Fig. (3). Braiding machine with (a) model diaphysis attached to the mandrel, (b) close up of the braided diaphysis, and (c) braided bone cast set with epoxy resin.

Table 1. Detailed Information of Each Braided Cast

Braid Number	Braid Angles (θ)	Number of Layers	Thickness
1	32°, 60°, 32°	3	1.8 mm
2	32°, 60°, 32°, 32°	4	2.0 mm
3	32°, 62.5°, 32°, 32°	4	2.2 mm

convergence to $\pm 1\%$ at 22390 nodes, which corresponded to an element size (the maximum element edge length [18]) of 2.5 mm. This element size was sufficient to produce convergence in the tubular and whole bone models as well.

Materials and Fabrication

Three synthetic humerus bones (model 3403) from Sawbones Worldwide (Pacific Research Laboratories, Inc., Washington, USA) designed to simulate the properties of human bone and provide less variable results were used in this experiment; these have been used in previous works for similar purposes [19]. The break was simulated by cutting a 20 mm gap in the middle of the diaphysis using a miter saw, which would be classified as a highly comminuted fracture likely to require internal fixation, based on the AO classification [16].

The braided socks were manufactured using a HS80-72 “IMC” Series braiding machine (Steegeer USA). The rotations per minute (RPM) and Picks per inch (PPI) settings were manipulated to produce the required braid angles (θ), defined from the longitudinal axis [20]. The external bone geometry of the synthetic humerus bone being tested was obtained using a Faro Arm 3 Foot Fusion laser scanner (FARO Technologies Inc.), and the computer programs Geomagic Studio 11 (Geomagic, Inc.) and Pro/Engineer Wildfire 5.0 (Parametric Technology Corp.) were used to manipulate the scanned model. This was rapid prototyped using the Objet Eden 350V (Objet Ltd.) to obtain a solid model of the humerus diaphysis. The model was secured

onto the mandrel to ensure that the exact bone geometry was braided. The braiding machine with the attached diaphysis model is shown in Fig. (3a) and (b).

The materials used in this experiment were Kevlar 49 fibers in a matrix of Cold Cure epoxy resin (Industrial Formulators Inc.). While these materials are not biocompatible over long periods [5, 21], they can serve as a basis to evaluate the concept; as well their material properties were readily available [22]. The epoxy was applied by hand, and the ends of the bone were held in place by a mould while the epoxy dried. Care was taken to ensure that the same amount of epoxy was applied to each braid and that the fibers were completely covered. Each cast was 125 mm long, centered on the missing section. An example of the braided bone cast applied to a synthetic humerus bone is shown in Fig. (3).

The detailed information of the composite bone casts is shown in Table 1, where the number and angle of braids were selected using the process outlined in the Theory/Calculation section.

Non-Destructive Testing

During testing, the distal ends of each humerus were secured inside a removable mould made of plastic (FullCure720), constructed using an Objet EDEN 350V rapid prototyper. This material was chosen due to its relatively high strength and modulus. Due to the identical physical properties of the synthetic bones, it allowed each bone to be held in precisely the same position. The mould was bolted onto wedges of different angles (20° and 60°

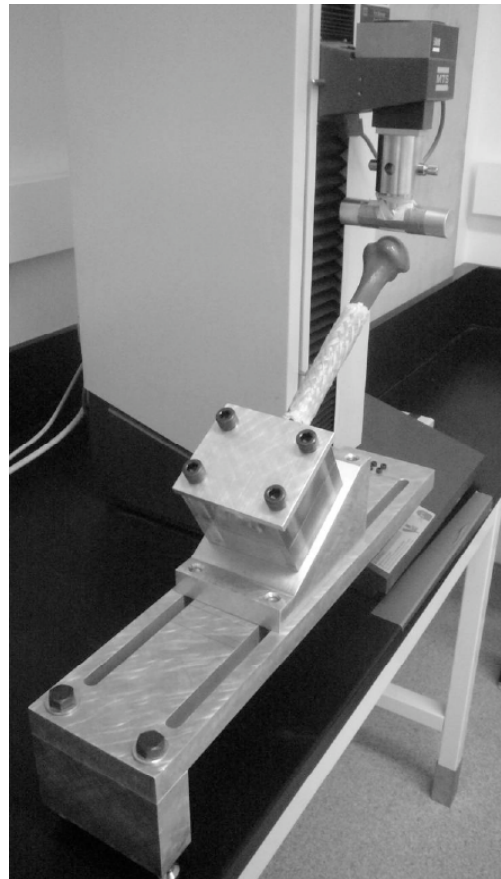


Fig. (4). Biomechanical test set-up, where the bones are secured using a rapid prototyped mould of the distal end of the humerus bolted into wedges of various angles.



Fig. (5). Schematic of three braids, each consisting of two layers.

abduction) required for testing, which allowed for testing a combination of bending and compression. The testing modes are similar to what have been used previously in literature [23].

Mechanical testing was performed using a Materials Testing System Synergie 400 testing machine (MTS Systems Corp.). A cylinder shaped indenter was used to apply the force to avoid unwanted stress concentrations at the point of contact. It was wrapped in a double layer of latex sheet to reduce slip. A cross-head speed of 100 mm/min was used for the 60° abduction tests, and 50 mm/min for the 20° abduction tests; the rapid loading rates minimized potential viscoelastic effects. The difference in cross-head speeds is a direct result of the fact that the cross-head cannot travel as far at 20° abduction, so at 100 mm/min, data acquisition was not fast enough to prevent the cross-head from exceeding the maximum desired load of 100 N. The set-up is shown in Fig. (4). A load of 100 N was chosen to ensure the bones did not

plastically deform, which allowed each specimen to serve as an internal control. Force displacement curves were generated for each of the three bones before and after casting, at angles of 20° and 60° abduction. Data was collected across 10 cycles of loading and unloading for each bone.

Theory/Calculation

Using Composite Laminate Plate Theory (CLPT), the braid angles and thickness were determined to produce elastic properties similar to bone, with shear stiffness higher than that of cortical bone. CLPT analysis is designed for predicting the properties of flat braids. Recent models have been developed to predict the properties of cylindrical braids [22], but the difference in properties was deemed negligible for the purpose of this validation. CLPT was used for the layering configuration shown in Fig. (5) [24]. Note that there were assumed to be two laminate layers per braid, each at opposite angles. Details of the CLPT analysis are shown in the appendix.

Table 2. Theoretical Braid Properties Based on CLPT Analysis

	* E_1	E_2	E_3	** G_{12}	G_{13}	G_{23}	*** ν_{21}	ν_{31}	ν_{32}
Cortical bone ^a	20.0	13.4	12.0	4.53	5.61	6.23	0.422	0.371	0.350
Braid 1	16.4	11.0	-	31.0	-	-	0.808	0.538	-
Braid 2	21.3	11.2	-	42.2	-	-	0.965	0.508	-
Braid 3	23.1	13.1	-	41.1	-	-	0.883	0.501	-

Note that directions 1, 2, and 3 are longitudinal, transverse and through the thickness, respectively.

^a – Refer to [17]

* E_i is elastic modulus (in GPa) in direction “i”.

** G_{ij} is the shear modulus (in GPa), where “i” is the normal direction of the plane and “j” is the shear direction along the plane.

*** ν_{ij} is the Poisson’s ratio (unitless).

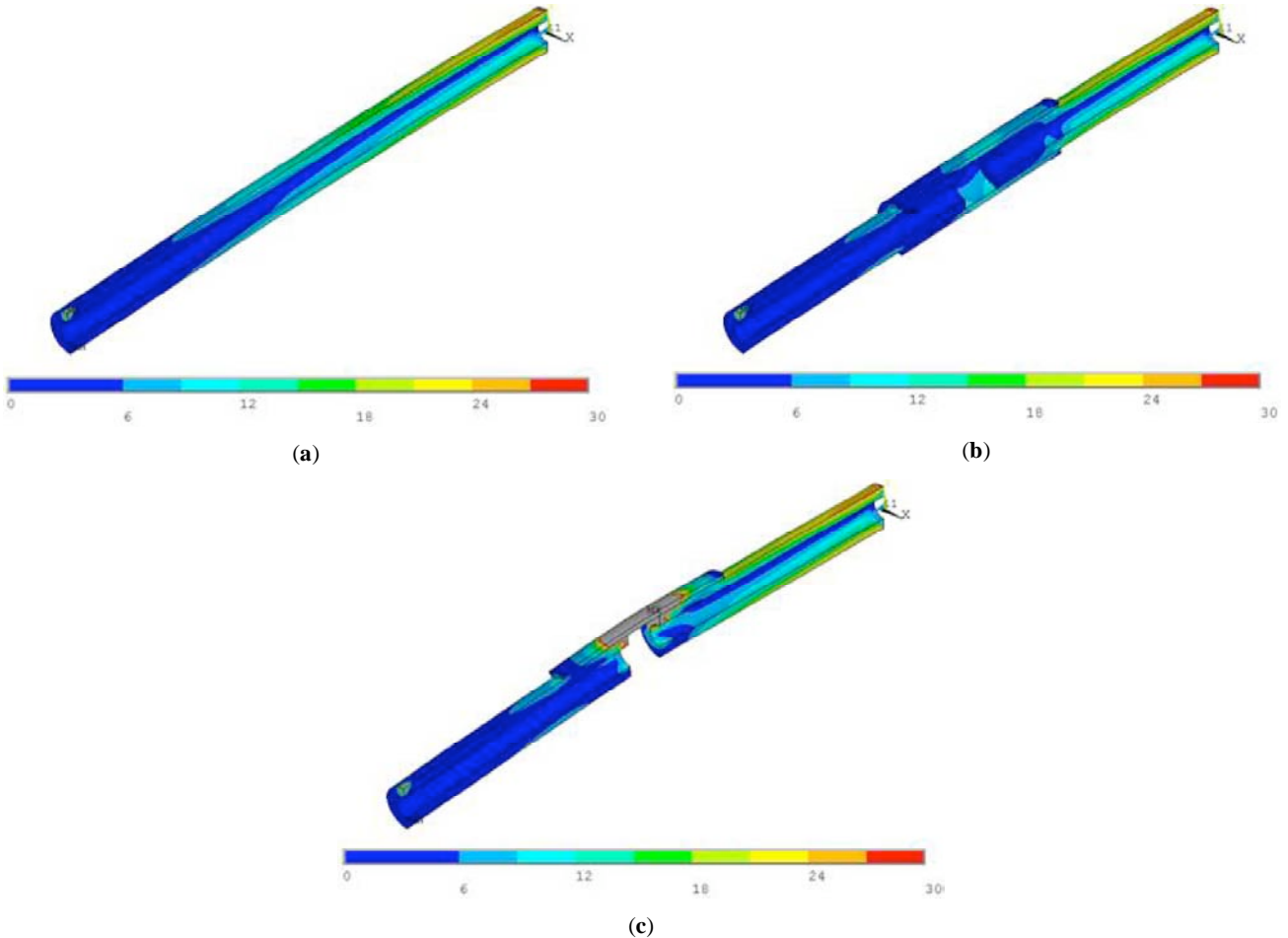


Fig. (6). Von Mises stress (in MPa) of (a) whole bone, (b) bone with tubular braid, and (c) bone with plate.

Various braid angle combinations were tested to attempt to match the elastic modulus to that of human cortical bone, as shown in Table 2. Directions 1, 2, and 3 are longitudinal, transverse and through the thickness, respectively. It was verified that the shear modulus was higher than bone.

RESULTS

Finite Element Analysis

The Von Mises stress was found at the same point in each model, at the edge of the fracture site centered directly under the cast. The maximum stress found in the intact bone was found to be 14.5 MPa. As expected, the plated cast resulted in much higher stresses, 111.3 MPa, than the

tubular, 6.8 MPa. This suggests that the tube is more able to distribute the stress evenly throughout the bone than the plate. It is also interesting to note that the tubular cast resulted in less stress in the bone than when uncasted. This would suggest that a thinner tube could be used, or a material with a lower stiffness. The Von Mises stress distributions are shown in Fig. (6), with contour plots ranging from 0 to 30 MPa.

It is clear that the stress distribution within the whole bone is more closely followed by the bone that was casted with the tube than with the plate. Again, this will promote healing following the principles of Wolf’s law. As well the stress concentrations present in the plated bone would result in uneven bone remodeling [10].

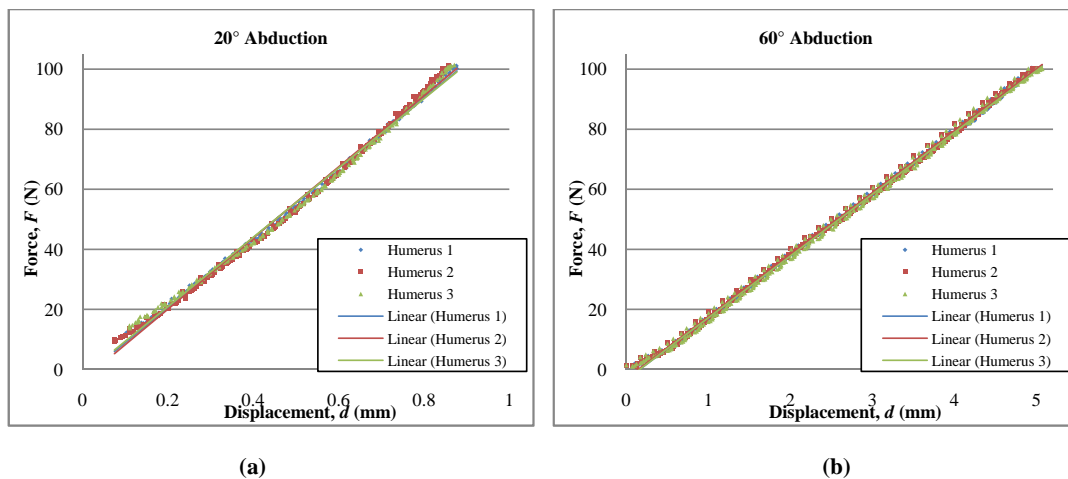


Fig. (7). Combination bending and compression force displacement graph of whole humeri held at (a) 20 degrees abduction, and (b) 60 degrees abduction.

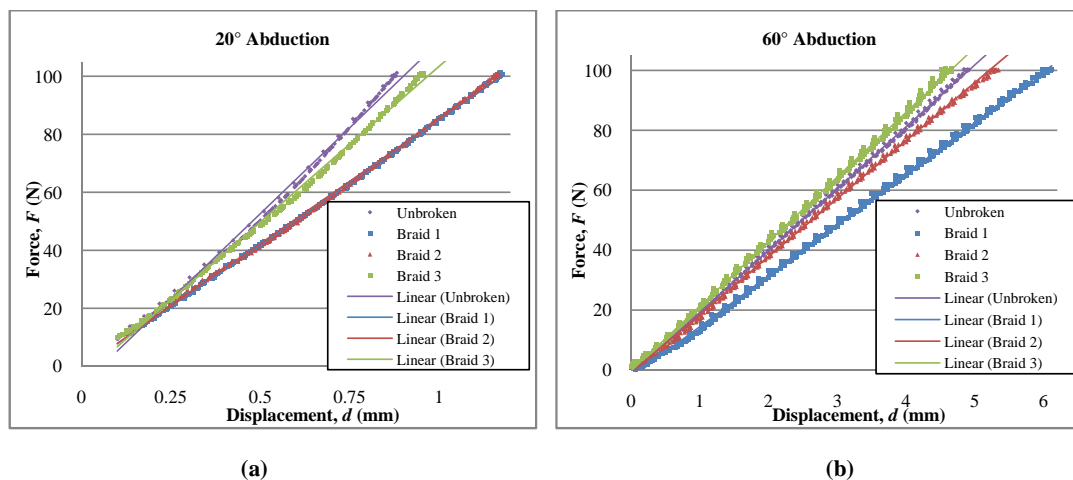


Fig. (8). Combination bending and compression force displacement graph of whole and broken humeri held at (a) 20° abduction, and (b) 60° abduction.

Unbroken Bones

The stiffness of each whole bone was found by taking the slope of the force displacement graphs using linear regression, as shown in Fig. (7). The average stiffnesses for the humeri at 20° abduction was 116.8 ± 1.5 N/mm, and 20.63 ± 0.02 N/mm at 60° abduction, where the standard deviation is found between bones.

The stiffness of each bone is very similar, thus it is clear that the difference in stiffness between each synthetic bone is negligible.

Braided Composite Repaired Bones

Each different combination of braid angles, as outlined in Table 1, produced different stiffnesses. The stiffnesses produced at 20° abduction for Braids 1, 2, and 3 were 85.8 ± 0.2 N / mm, 83.0 ± 0.1 N / mm, and 107.4 ± 0.3 N / mm respectively. At 60° abduction the stiffnesses were 17.02 ± 0.06 N / mm, 19.36 ± 0.03 N / mm, and 21.59 ± 0.15 N / mm respectively. The standard deviations are found across ten trials of loading each bone. A graphical comparison is shown in Fig. (8). The stiffnesses increased as additional braid layers were added, as well as when the internal angle was increased from 60° to 62.5°.

In each case, the third bone casted in each test was within 10% stiffness of the whole bone. At 20° abduction, the whole bone stiffness was 8.0% higher, and at 60° whole bone stiffness was 4.7% lower. The first two casted bones produced stiffnesses lower than the whole bone at both angles measured.

DISCUSSION

Braided casts have been investigated as a potential replacement for compression bone plates. This is due to the many disadvantages associated with plates previously outlined. The objective of this investigation was to demonstrate the proof of this concept by testing synthetic bones. It was hypothesized that the cast would give the broken bone properties similar to normal bone.

Based on the work done with the simplistic FEA model, it is clear that a tubular cast would produce less stress concentrations in the fractured ends of the bone than a plate. The reduction in stress concentration is desirable, since a more even stress distribution will result in reduced bone remodeling over the fracture site [10]. Additionally, a thinner tubular cast could be used, which is desirable due to the

limited space between muscle and bone [14]. The tubular cast has been shown to be a promising fixation method for healing broken bones.

In a FEA study conducted by Haase *et al.* [25], a bone was placed under a bending load of 125 N·m to simulate a four point bending test, and the stress in the bone underneath the plate was calculated. The resultant stress found in the bone directly under the plate was approximately 400 MPa, compared to the 111 MPa found in this study. Considering the differences between model set-ups, the similarity suggests a valid model.

A search through the literature did not reveal studies into the effects of a tubular bone cast, although Lin *et al.* found that larger separation angles (90° versus 50°) between bone plates result in a more even stress distribution [26]; that the more evenly spaced the cast, the more evenly spaced the stress distribution. This follows the results found in this study, in that a tube is more evenly spaced around a bone than a plate.

Experimental work showed that the average stiffnesses for the unbroken humeri at 20° abduction were calculated to be 116.8 ± 1.5 N/mm, and 20.63 ± 0.02 N/mm at 60° abduction. In the experiment performed by Lever *et al.* (which used a similar testing method), 25 whole cadaveric bones held at 20° abduction had stiffnesses ranging from 62.6 ± 25.0 to 197.6 ± 31.6 N/mm [27]. These large ranges are likely due to different types of bone specimens being used in the cadaver experiment; age, gender, and usage are among many factors that can heavily influence bone geometry and density, two properties that are closely linked to overall stiffness [15]. Comparison of the results is very encouraging for the proposed casting method.

Each of the three unbroken bones tested produced very similar stiffness properties, which follow published experimental results. This would suggest that the use of Sawbones synthetic bones is beneficial in that they are able to correctly simulate the properties of real bones, and they can be used to yield reproducible results, as previously demonstrated [28]. Synthetic bones are easier to obtain and handle than cadaveric bones, and so allow for more testing to be completed. As well there is less variability which produces results that are easier to interpret and have been used for in-vitro testing previously [19, 29].

It has been shown that the braid angle and thickness of a tubular cast can be tailored to produce stiffnesses similar to those of whole, unbroken bone. While the exact stiffness was not obtained (due to resource limitations), the stiffnesses of the broken bones at both 60° and 20° abduction were within 10% of the desired stiffness of the unbroken bones. This is a promising result, since the stress shielding effect would be reduced so more effective bone repair would be possible [2-4].

In the future, further investigation will focus on using different braid angles, thicknesses, and lengths to attempt to match the casted bone stiffness to the original bone stiffness. Different angles of force application should be tested, as well as different loading scenarios such as torsion. Unfortunately, fatigue cannot be adequately tested, since the biological repair process cannot be simulated [23]. FEA could be used to further investigate this method using more accurate bone geometries and material properties, as well as modeling the braided composite.

One of the main concerns for this project is finding biocompatible and biodegradable materials. While suture materials are biocompatible, and some are resorbable, they are not strong enough to be used for this application [30]. Several different resins show potential for biocompatibility, including hydroxyapatite [31], PRISMA VLC DYCAL [32], and methyl methacrylate [3]. Other researchers suggest that further investigation into the long term effects of contact with resin is required [33]. Several different biocompatible bone plates have been found to have material properties similar to bone. One is the braided carbon/PEEK plate studied by Fujihara *et al.* [14]. This type of bone plate would not be resorbable, since carbon fibres are not biocompatible over extended periods of time, but rather would require “fully matrix covered surfaces” [12]. As such, an additional surgery would be required to remove the plate once the bone was healed. Research has been conducted regarding a composite bone plate containing Poly L-Lactic acid matrix and textile bioglass fibers, and has been found to be partially resorbable [34]. This promising research demonstrates that there are materials available that are biocompatible and may be useable for manufacturing the braided tubular cast.

The results demonstrated in this paper are very promising. FEA was used to show that a tubular cast results in less stress concentrations in the fractured ends of the bone than a plate, which would assist with healing. The cast would be able to contain small bone fragments, which could help with the healing process. As well the need for screws would be eliminated. It was shown that the braid angle and thickness of the tubular cast could be tailored to produce stiffnesses similar to those of whole, unbroken bone. A brief review of potential materials was presented, and further research possibilities were discussed. The composite braided cast has shown to be both feasible and promising for the treatment of broken bones.

LIST OF ABBREVIATIONS

^F EA	=	finite element analysis
AO	=	Swiss Association for the Study of Problems of Internal Fixation
RPM	=	rotations per minute
PPI	=	picks per inch
CLPT	=	composite laminate plate theory

CONFLICT OF INTEREST

This work has no financial relationship that may pose a conflict of interest.

ACKNOWLEDGMENTS

The authors wish to acknowledge Dr. Richard Ng, MD for his insight. Authors acknowledge the funding from Natural Sciences and Engineering Research Council of Canada and TecEdmonton for equipment.

APPENDIX

For the following calculations, note that direction 1 is along fibre direction and direction 2 is perpendicular to fibre direction.

First, the elastic moduli of the composite in directions 1 and 2 were found using the Rule of Mixing and the Rule of Reciprocal, respectively.

$$E_1 = E_f \cdot V_f + E_m(1 - V_f) \quad (1)$$

$$E_2 = \left(\frac{V_f}{E_f} + \frac{1-V_f}{E_m} \right)^{-1} \quad (2)$$

Here, E_f (130 GPa) and E_m (0.376 GPa) are the elastic moduli of the fibre and matrix (in GPa), respectively, V_f (0.60) is the volume fraction of fibre as compared to matrix, and E_1 and E_2 are the elastic moduli in the fibre direction (in GPa), and perpendicular to the fibre direction, respectively.

The shear modulus was found using the Rule of Reciprocal.

$$G_{12} = \left(\frac{V_f}{G_f} + \frac{1-V_f}{G_m} \right)^{-1} \quad (3)$$

Where G_f (2.86 GPa), G_m (0.145 GPa), and G_{12} are the shear moduli of the fibre, the matrix, and the composite, respectively (in GPa).

The Poisson's ratio was found in each direction, using the Rule of Mixing.

$$\nu_{12} = \nu_f \cdot V_f + \nu_m(1 - V_f) \quad (4)$$

$$\nu_{21} = E_2 \frac{\nu_{12}}{E_1} \quad (5)$$

Where ν_f (0.35), ν_m (0.30), ν_{12} , and ν_{21} are the Poisson's ratios of the fibre, the matrix, the composite in the fibre direction, and perpendicular to the fibre direction, respectively.

Note that there were assumed to be two laminate layers per braid, each at opposite angles and with a thickness of t (in mm). Each braid angle was chosen, and transformed stiffness matrices were calculated. First, the stiffness matrix was formed (in Pa).

$$Q = \begin{bmatrix} Q_{11} & Q_{12} & 0 \\ Q_{12} & Q_{22} & 0 \\ 0 & 0 & Q_{66} \end{bmatrix} \quad (6)$$

$$Q_{11} = \frac{E_1}{1-\nu_{12}\nu_{21}} \quad (7)$$

$$Q_{22} = \frac{E_2}{1-\nu_{12}\nu_{21}} \quad (8)$$

$$Q_{12} = \nu_{12} \frac{E_2}{1-\nu_{12}\nu_{21}} \quad (9)$$

$$Q_{66} = G_{12} \quad (10)$$

The transformation matrix was formed for each braid angle (θ) chosen.

$$T(\theta) = \begin{bmatrix} \cos^2(\theta) & \sin^2(\theta) & 2\sin(\theta) \cdot \cos(\theta) \\ \sin^2(\theta) & \cos^2(\theta) & -2\sin(\theta) \cdot \cos(\theta) \\ -\sin(\theta) \cdot \cos(\theta) & \sin(\theta) \cdot \cos(\theta) & \cos^2(\theta) - \sin^2(\theta) \end{bmatrix} \quad (11)$$

Then the transformed stiffness matrix in each direction was calculated.

$$\bar{Q} = T^{-1}(\theta) \cdot Q \cdot T(\theta) \quad (12)$$

Using these matrices, the extensional stiffness matrix was formed, assuming that the thickness of each braid layer was constant.

$$A = \sum_0^i Q_i [d_{lower} - d_{upper}] = \sum_0^i Q_i t \quad (13)$$

Finally the material properties of the composite braid were determined. Note that the x denotes the absolute longitudinal direction, and y the absolute transverse direction. The elastic modulus was found.

$$E_x = \frac{A_{1,1} \cdot A_{2,2} - A_{1,2}^2}{A_{2,2} \cdot 6t} \quad (14)$$

$$E_y = \frac{A_{1,1} \cdot A_{2,2} - A_{1,2}^2}{A_{1,1} \cdot 6t} \quad (15)$$

Next the Poisson's ratio was calculated.

$$\nu_{xy} = \frac{A_{1,2}}{A_{2,2}} \quad (16)$$

$$\nu_{yx} = \frac{A_{1,2}}{A_{1,1}} \quad (17)$$

Finally, shear modulus was calculated.

$$G_{xy} = \frac{A_{1,2}}{6t} \quad (18)$$

REFERENCES

- [1] Kutz, *Standard handbook of biomedical engineering & design*. Toronto: McGraw-Hill, 2003.
- [2] G. W. Bradley, G. B. McKenna, H. K. Dunn, A. U. Daniels, and N. Statton, 'Effects of flexural rigidity of plates on bone healing', *J. Bone Joint Surg.*, vol. 61, pp. 866-872, 1979.
- [3] S. Woo, W. H. Akeson, B. Levenetz, R. D. Coutts, J. V. Matthews, and D. Amiel, 'Potential application of graphite fiber and methyl methacrylate resin composites as internal fixation plates', *J. Biomed. Mater. Res.*, vol. 8, no. 5, pp. 321-338, 1974.
- [4] W. H. Akeson, S. L.-Y. Woo, R. D. Coutts, J. V. Matthews, M. Gonsalves, and D. Amiel, 'Quantitative histological evaluation of early fracture healing of cortical bones immobilized by stainless steel and composite plates', *Calcif. Tissue Res.*, vol. 19, no. 1, pp. 27-37, 1975.
- [5] S. Ramakrishna, J. Mayer, E. Wintermantel, and K. W. Leong, 'Biomedical applications of polymer-composite materials: a review', *Compos. Sci. Technol.*, vol. 61, no. 9, pp. 1189-1224, 2001.
- [6] P. A. Deluca, R. W. Lindsey, and X. Ruwe, 'Refracture of bones of the forearm after the removal of compression plates', *J. Bone Joint Surg.*, vol. 70, pp. 1372-1376, 1988.
- [7] H. Schell, D. R. Epari, J. P. Kassi, H. Bragulla, H. J. Bail, and G. N. Duda, 'The course of bone healing is influenced by the initial shear fixation stability', *J. Orthopaed. Res.*, vol. 23, no. 5, pp. 1022-1028, 2005.
- [8] P. Augat, J. Burger, S. Schorlemmer, T. Henke, M. Peraus, and L. Claes, 'Shear movement at the fracture site delays healing in a diaphyseal fracture model', *J. Orthop. Res.*, vol. 21, no. 6, pp. 1011-1017, Nov. 2003.
- [9] Z. Huang and K. Fujihara, 'Stiffness and strength design of composite bone plates', *Compos. Sci. Technol.*, vol. 65, pp. 73-85, 2005.
- [10] J. A. Szivek, G. C. Weatherly, R. M. Pilliar, and H. U. Cameron, 'A study of bone remodeling using metal-polymer laminates', *J. Biomed. Mater. Res.*, vol. 15, no. 6, pp. 853-865, 1981.
- [11] K. Fujihara, K. Teo, R. Gopal, P. L. Loh, V. K. Ganesh, S. Ramakrishna, K. W. C. Foong, and C. L. Chew, 'Fibrous composite materials in dentistry and orthopaedics: review and applications', *Compos. Sci. Technol.*, vol. 64, no. 6, pp. 775-788, 2004.
- [12] E. Wintermantel, J. Mayer, and T. N. Goehring, 'Composites for biomedical applications', *Encyclopedia of materials: Science and technology*, vol. 2 C, Elsevier Science Ltd: Oxford, UK, pp. 1371-1376, 2001.

- [13] Y. Z. Wan, Y. L. Wang, F. He, Y. Huang, and H. J. Jiang, 'Mechanical performance of hybrid bismaleimide composites reinforced with three-dimensional braided carbon and Kevlar fabrics', *Composites Part A*, vol. 38, no. 2, pp. 495-504, 2007.
- [14] K. Fujihara, Z. M. Huang, S. Ramakrishna, K. Satknanantham, and H. Hamada, 'Performance study of braided carbon/PEEK composite compression bone plates', *Biomaterials*, vol. 24, no. 15, pp. 2661-2667, 2003.
- [15] K. Fujihara, Z. M. Huang, S. Ramakrishna, K. Satknanantham, and H. Hamada, 'Feasibility of knitted carbon/PEEK composites for orthopedic bone plates', *Biomaterials*, vol. 25, no. 17, pp. 3877-3885, 2004.
- [16] M. Müller, P. Koch, S. Nazarian, and J. Schatzker, *The Comprehensive Classification of Fractures of Long Bones*. Germany: Springer-Verlag Berlin Heidelberg, 1990.
- [17] R. B. Ashman, S. C. Cowin, W. C. Van Buskirk, and J. C. Rice, 'A continuous wave technique for the measurement of the elastic properties of cortical bone', *J. Biomech*, vol. 17, no. 5, pp. 349-361, 1984.
- [18] ANSYS. SAS IP, Inc., 2009.
- [19] A. C. M. Chong, E. A. Friis, G. P. Ballard, P. J. Czuwala, and F. W. Cooke, 'fatigue performance of composite analogue femur constructs under high activity loading', *Ann. Biomed. Eng.*, vol. 35, no. 7, pp. 1196-1205, 2007.
- [20] J. Carey, M. Munro, and A. Fahim, 'Regression-based model for elastic constants of 2D braided/woven open mesh angle-ply composites', *Polym. Compos.*, vol. 26, no. 2, pp. 152-164, 2005.
- [21] R. F. Storey, J. S. Wiggins, K. A. Hogan, and A. D. Puckett, 'Bioabsorbable composites. I: Fundamental design considerations using free radically crosslinkable matrices', *Polym. Compos.*, vol. 14, no. 1, pp. 7-16, 1993.
- [22] C. Ayranci and J. P. Carey, 'Predicting the longitudinal elastic modulus of braided tubular composites using a curved unit-cell geometry', *Compos. Part B*, vol. 41, no. 3, pp. 229-235, 2010.
- [23] K. J. Koval, B. Blair, R. Takei, F. J. Kummer, and J. D. Zuckerman, 'Surgical neck fractures of the proximal humerus: a laboratory evaluation of ten fixation techniques', *J. Trauma*, vol. 40, no. 5, pp. 778-783, 1996.
- [24] B. D. Agarwal and L. J. Broutman, *Analysis and performance of fiber composites*. Wiley, 1990.
- [25] K. Haase and G. Rouhi, 'A discussion on plating factors that affect stress shielding using finite element analysis.pdf', *J. Biomech. Sci. Eng.*, vol. 5, no. 2, pp. 129-141, 2010.
- [26] C. L. Lin, Y. H. Lin, and A. C. Y. Chen, 'Buttressing angle of the double-plating fixation of a distal radius fracture: a finite element study', *Med. Bio. Eng. Comput.*, vol. 44, no. 8, pp. 665-673, 2006.
- [27] J. P. Lever, S. A. Aksenov, R. Zdero, H. Ahn, M. D. McKee, and E. H. Schemitsch, 'Biomechanical analysis of plate osteosynthesis systems for proximal humerus fractures', *J. Orthop. Trauma*, vol. 22, no. 1, pp. 23-29, 2008.
- [28] J. T. Dunlap, A. C. M. Chong, G. L. Lucas, and F. W. Cooke, 'structural properties of a novel design of composite analogue humeri models', *Ann. Biomed. Eng.*, vol. 36, pp. 1922-1926, Sep. 2008.
- [29] R. Zdero, M. Olsen, H. Bougherara, and E. H. Schemitsch, 'Cancellous bone screw purchase: a comparison of synthetic femurs, human femurs, and finite element analysis', *J. Eng. Med.*, vol. 222, no. 8, pp. 1175-1183, 2008.
- [30] J. Elsner and M. Zilberman, 'Antibiotic-eluting bioresorbable composite fibers for wound healing applications: microstructure, drug delivery and mechanical properties', *Acta Biomater.*, vol. 5, no. 8, pp. 2874-2883, 2009.
- [31] P. S. Stein, J. Sullivan, J. E. Haubenreich, and P. B. Osborne, 'Composite resin in medicine and dentistry', *J. Long Term Eff. Med. Implants*, vol. 15, no. 6, pp. 641-654, 2005.
- [32] P. D. Hammesfahr, 'Biocompatible resins in dentistry', *J. Biomater. Appl.*, vol. 1, pp. 373-381, 1986.
- [33] S. Bouillaguet, L. Shaw, L. Gonzalez, J. C. Wataha, and I. Krejci, 'Long-term cytotoxicity of resin-based dental restorative materials', *J. Oral. Rehabil.*, vol. 29, no. 1, pp. 7-13, 2002.
- [34] A. Zargar Kharazi, M. H. Fathi, and F. Bahmany, 'Design of a textile composite bone plate using 3D-finite element method', *J. Mater. Des.*, vol. 31, pp. 1468-1474, 2009.

Received: September 11, 2012

Revised: November 08, 2012

Accepted: November 28, 2012

© Evans and Carey; Licensee Bentham Open.

This is an open access article licensed under the terms of the Creative Commons Attribution Non-Commercial License (<http://creativecommons.org/licenses/by-nc/3.0/>) which permits unrestricted, non-commercial use, distribution and reproduction in any medium, provided the work is properly cited.